Supplementary Information for

Insights into the First Multi-Transition-Metal Containing Ruddlesden Popper-Type Cathode for all-solid-state Fluoride Ion Batteries

Vanita Vanita [a], Aamir Iqbal Waidha [a], Sami Vasala [b], Pascal Puphal [d], Roland Schoch [c], Pieter Glatzel [b], Matthias Bauer [c], & Oliver Clemens [a*]

[a] University of Stuttgart, Institute for Materials Science, Materials Synthesis Group, Heisenbergstraße 3, 70569 Germany

[b] ID26, European Synchrotron Radiation Facility (ESRF), 71 avenue des Martyrs CS 40220, 38043 Grenoble Cedex 9

[c] Institute of Inorganic Chemistry and Center for Sustainable Systems Design (CSSD), Paderborn University, Warburger Straße 100, 33098 Paderborn, Germany.

[d] Max-Planck-Institute, Heisenbergstr. 1, 70569 Stuttgart, Germany

* Corresponding Author:

Prof. Dr. Oliver Clemens

Email: oliver.clemens@imw.uni-stuttgart.de

Fax: +49 711 685 51933

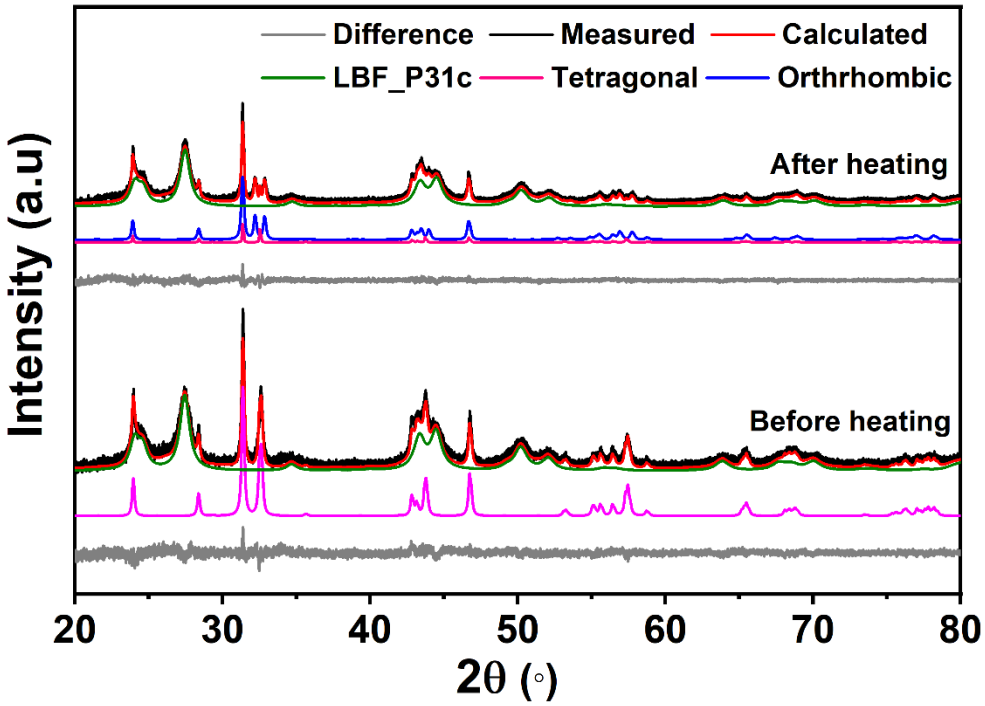

Figure S 1. XRD of cathode material before and after heating at T= 170°C.

Table S 1. Details of the structures of the pristine, cathode material and after heating the cathode material at T= 170°C

		$La_2Ni_{0.75}Co_{0.25}O_{4.08}$	**Cathode composite**	**Heated cathode composite**
Crystal system and space group		Tetragonal I4/mmm	Tetragonal I4/mmm	Tetragonal I4/mmm
Lattice parameter	a	3.88125(4)	3.88081(19)	3.88088(19)
	c	12.57064(18)	12.5688(9)	12.5690(9)
Cell volume		189.365(4) ($Å^3$)	189.30(2) ($Å^3$)	189.30(2)

Table S 2. $La_2Ni_{0.75}Co_{0.25}O_{4.08}$ Weight and Atomic % from the EDAX analysis

Element	Weight %	Atomic %
La L	73.10	33.80
Ni K	11.10	12.10
Co K	04.40	04.80
O K	08.90	35.70

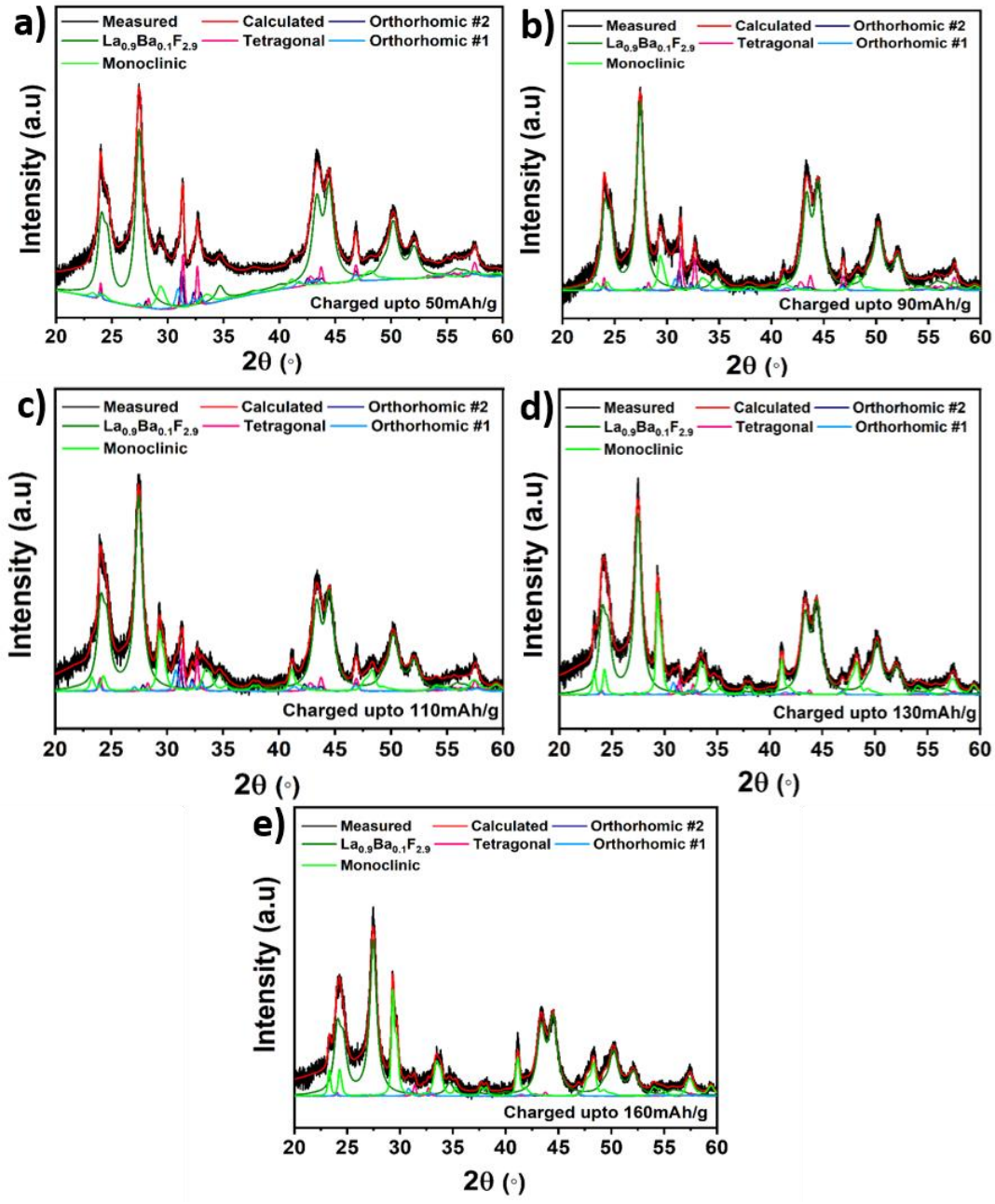

Figure S 2. ***Structural changes of the RP-type phase at different cut off capacities.*** *Retiveld refinement for* $La_2Ni_{0.75}Co_{0.25}O_{4.08}$ */Pb-PbF2 at T=170 dc,* I_{charge}*=+8.0294uA,* $I_{discharge}$*= -4.0145uA, at the charging capcacity of (a) 50 mAh* g^{-1} *(b) 90 mAh* g^{-1} *(c) 110 mAh* g^{-1} *(d) 130 mAh* g^{-1} *(e) 160 mAh* g^{-1}

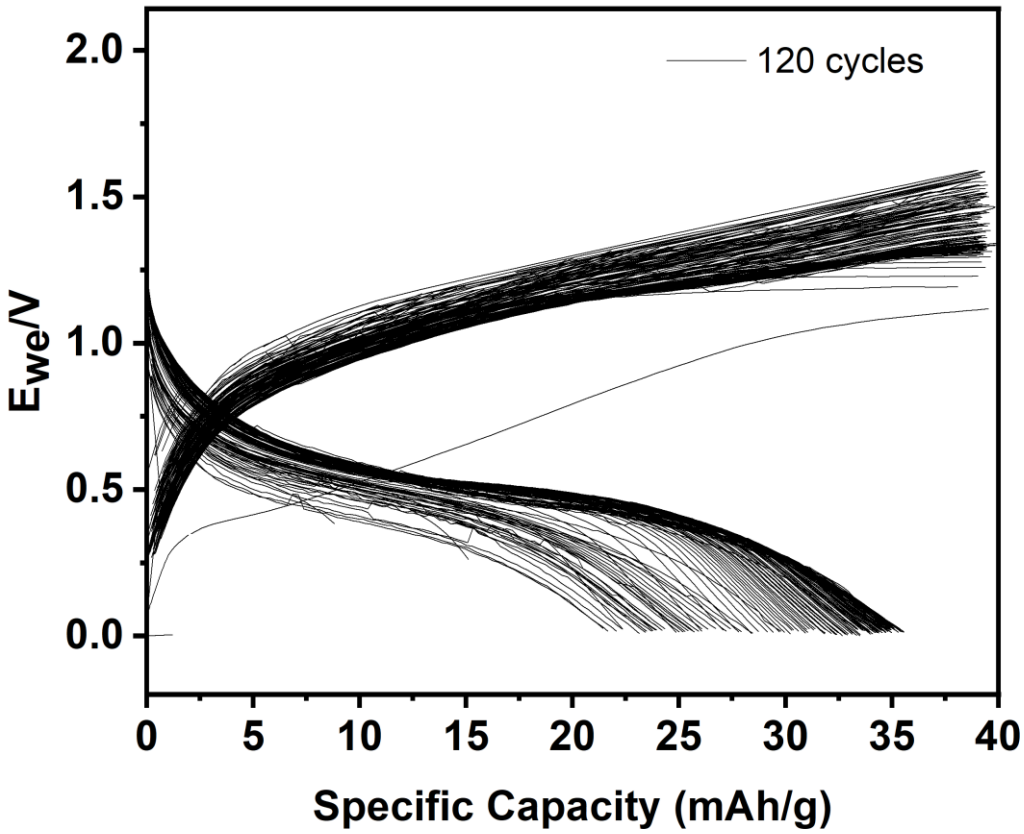

Figure S 3. Capacity-voltage curves for the cell operated for 120 cycles between 0 and 1.5 V

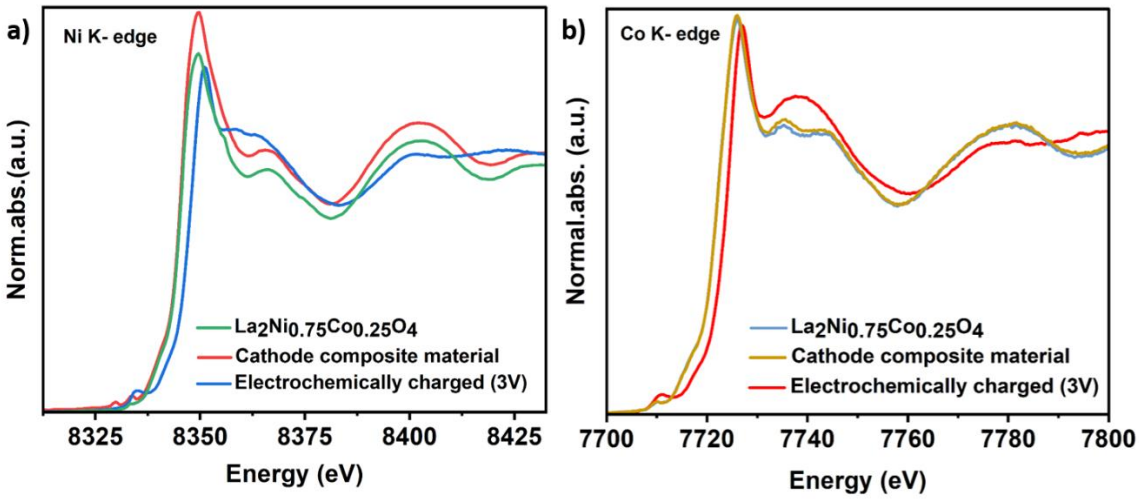

Figure S 4. The absorption edge energies of $La_2Ni_{0.75}Co_{0.25}O_{4.08}$ compared to cathode composite of $La_2Ni_{0.75}Co_{0.25}O_{4.08}$ and electrochemically charged upto 3V at Ni, Co K-edge.

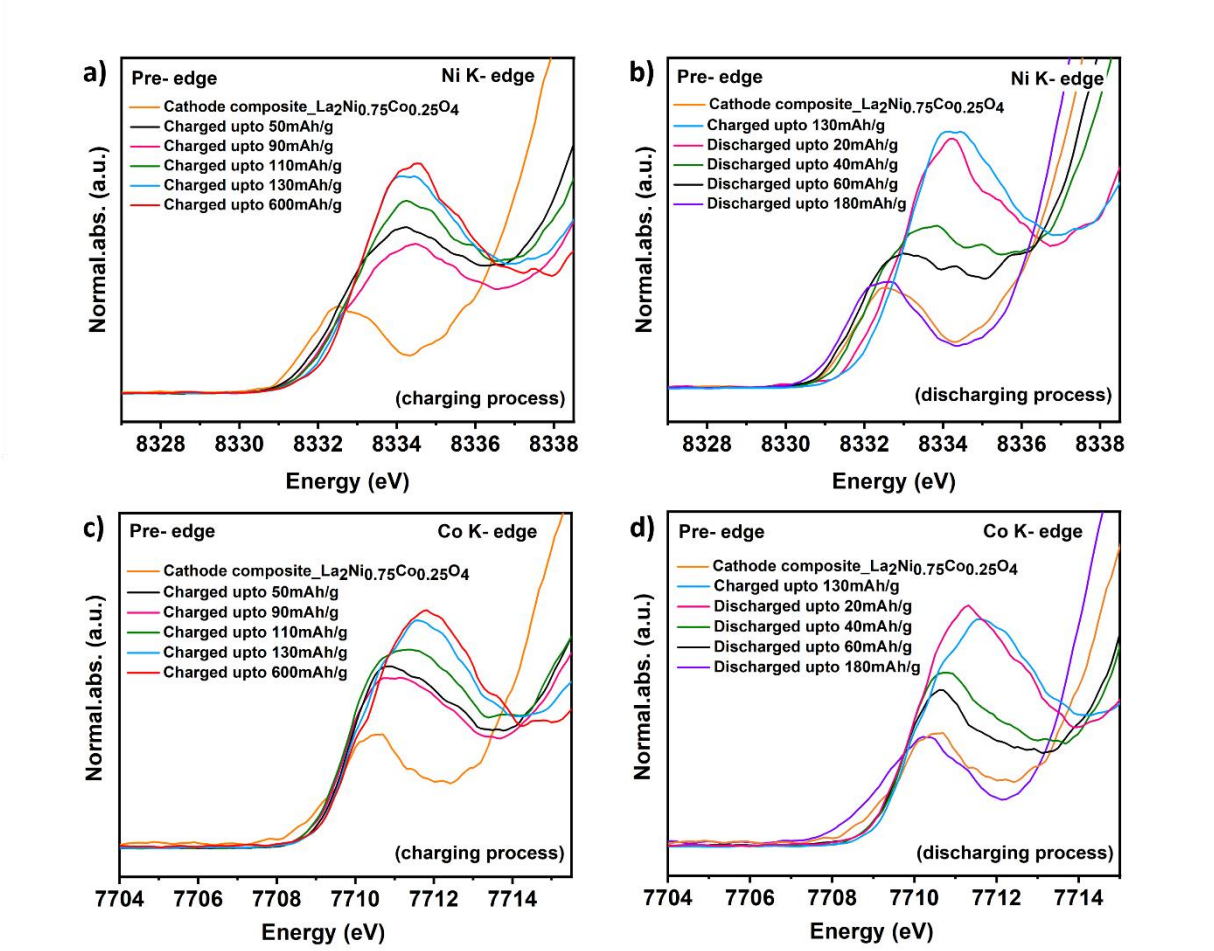

Figure S 5. Pre- edge of HERFD- XAS at Ni K-edge (a) $La_2Ni_{0.75}Co_{0.25}O_{4.08}$ after F^- insertion (b) $La_2Ni_{0.75}Co_{0.25}O_{4.08}$ after F^- extraction Pre- edge at Co K-edge (c) $La_2Ni_{0.75}Co_{0.25}O_{4.08}$ after F^- insertion (d) $La_2Ni_{0.75}Co_{0.25}O_{4.08}$ after F^- extraction.

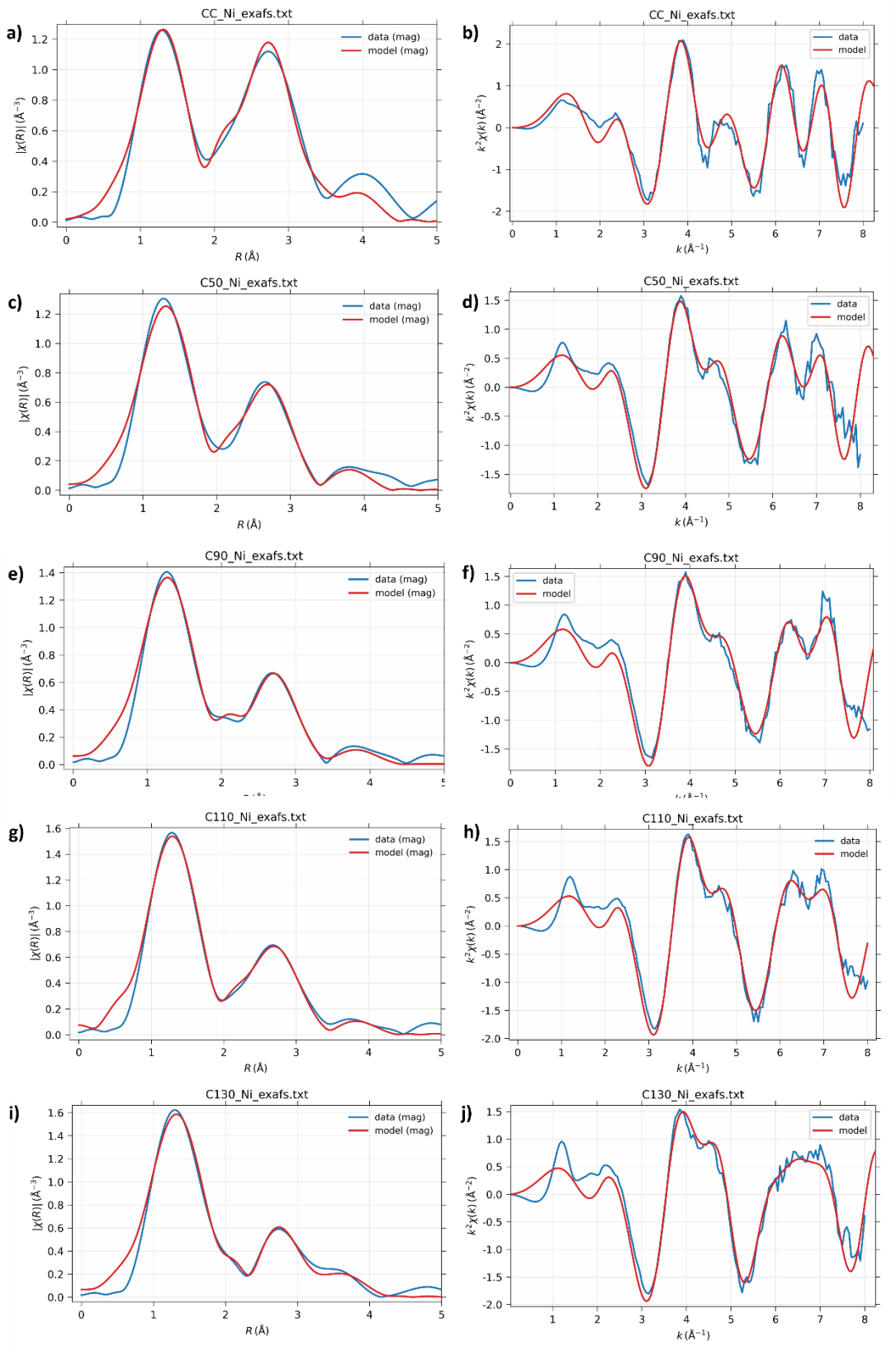

Figure S 6. EXAFS fits in R and k space at Ni K-edge of $La_2Ni_{0.75}Co_{0.25}O_{4.08}$ after F^- insertion.

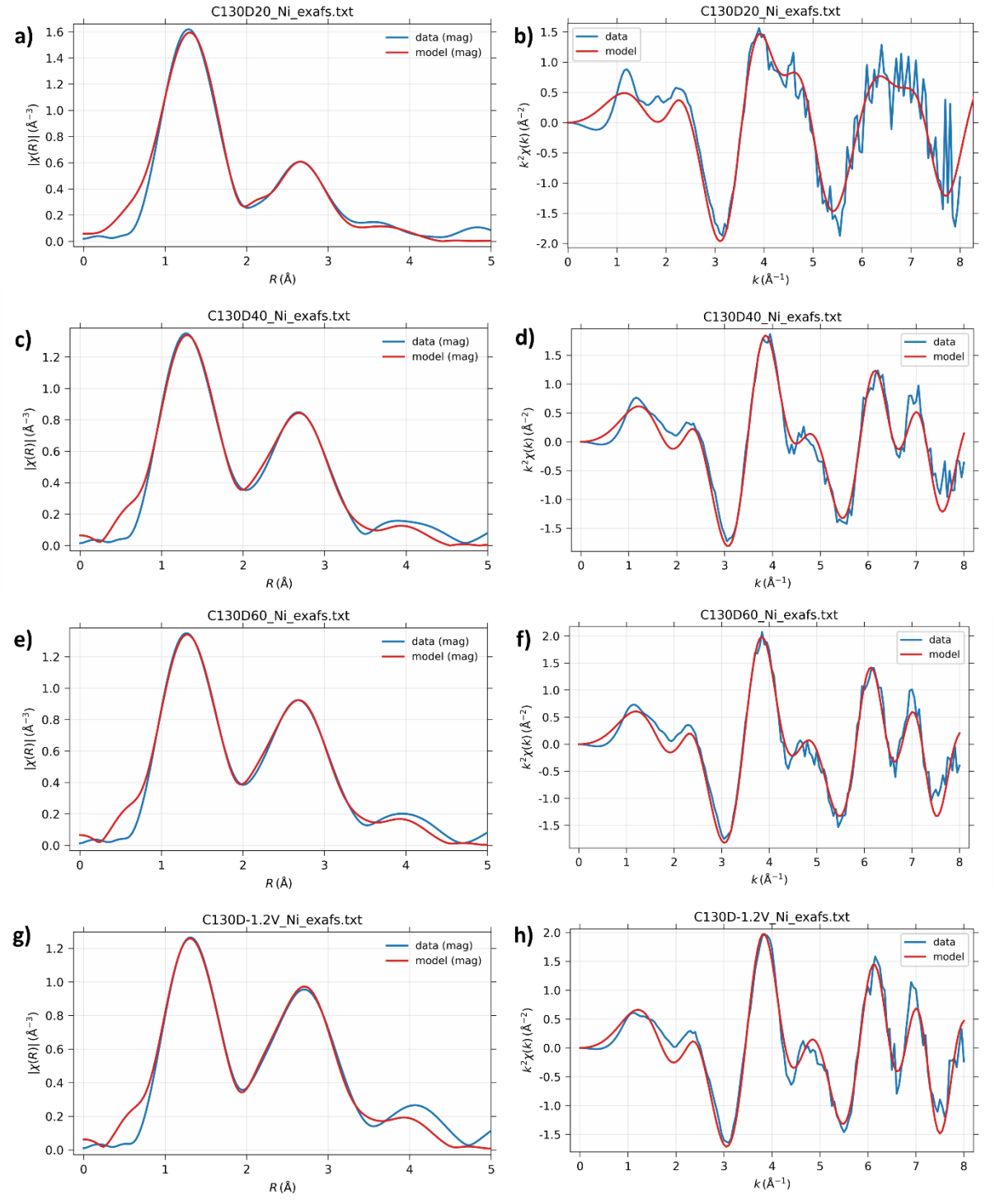

Figure S 7. EXAFS fits in R and k space at Ni K-edge of $La_2Ni_{0.75}Co_{0.25}O_{4.08}$ after F^- extraction.

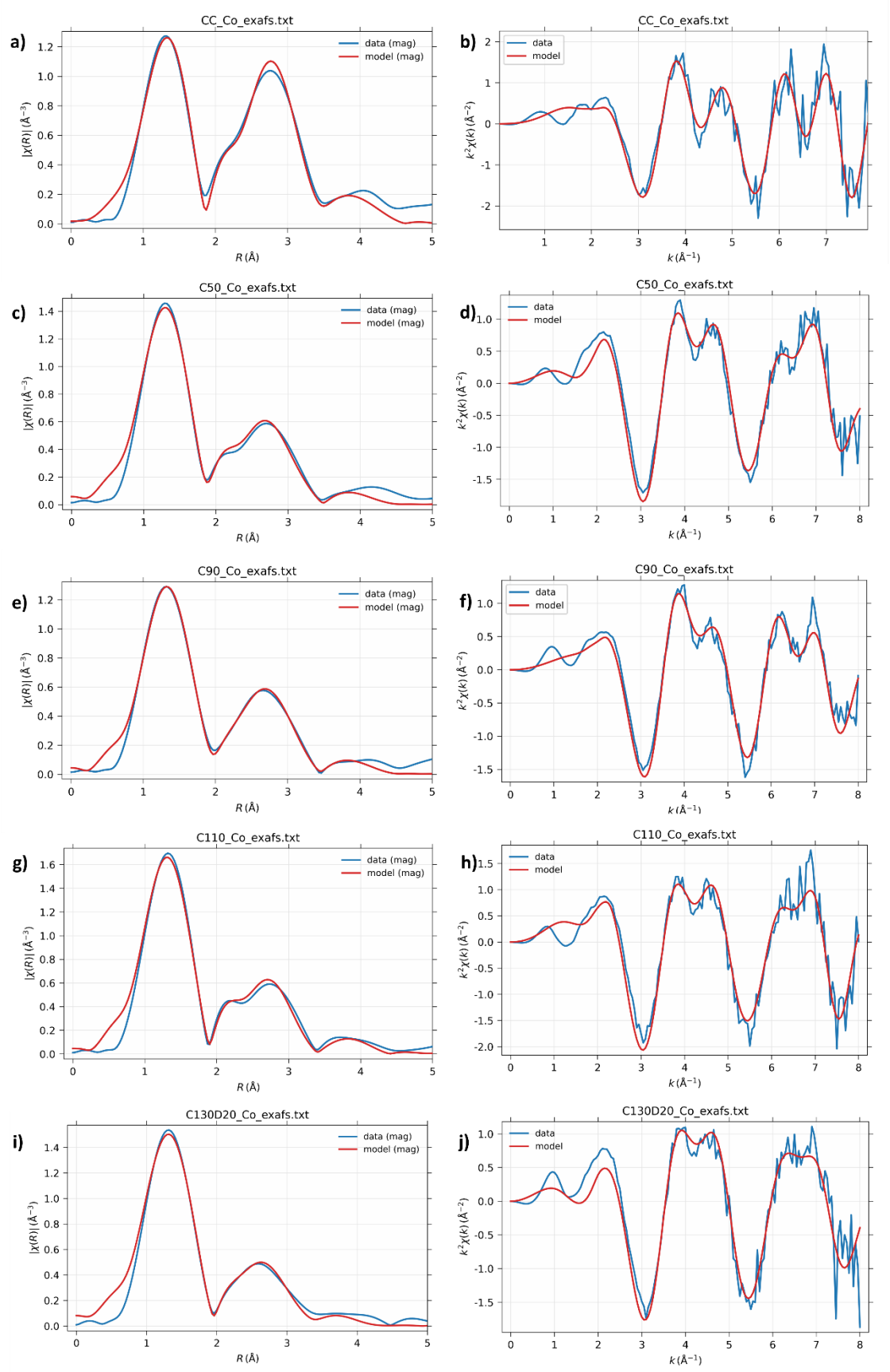

Figure S 8. EXAFS fits in R and k space at Co K-edge of $La_2Ni_{0.75}Co_{0.25}O_{4.08}$ after F^- insertion.

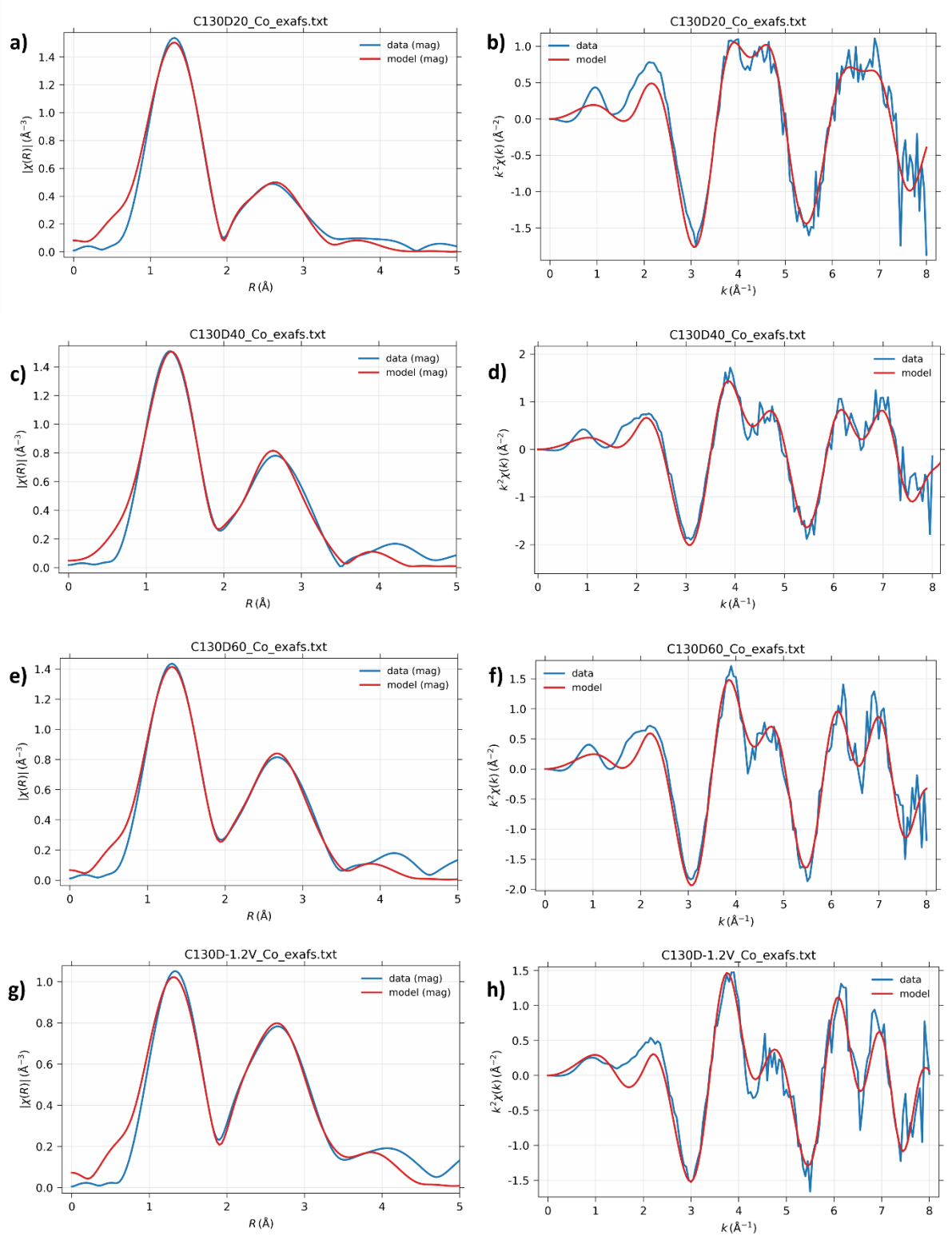

Figure S 9. EXAFS fits in R and k space at Co K-edge of $La_2Ni_{0.75}Co_{0.25}O_{4.08}$ after F^- extraction.

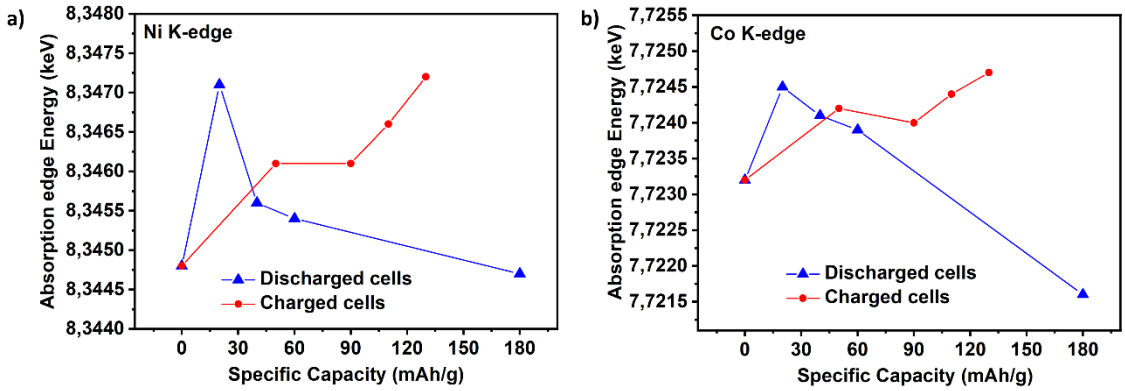

Figure S 10. Adsorption energies shift of $La_2Ni_{0.75}Co_{0.25}O_{4.08}$ during F^- insertion and extraction.

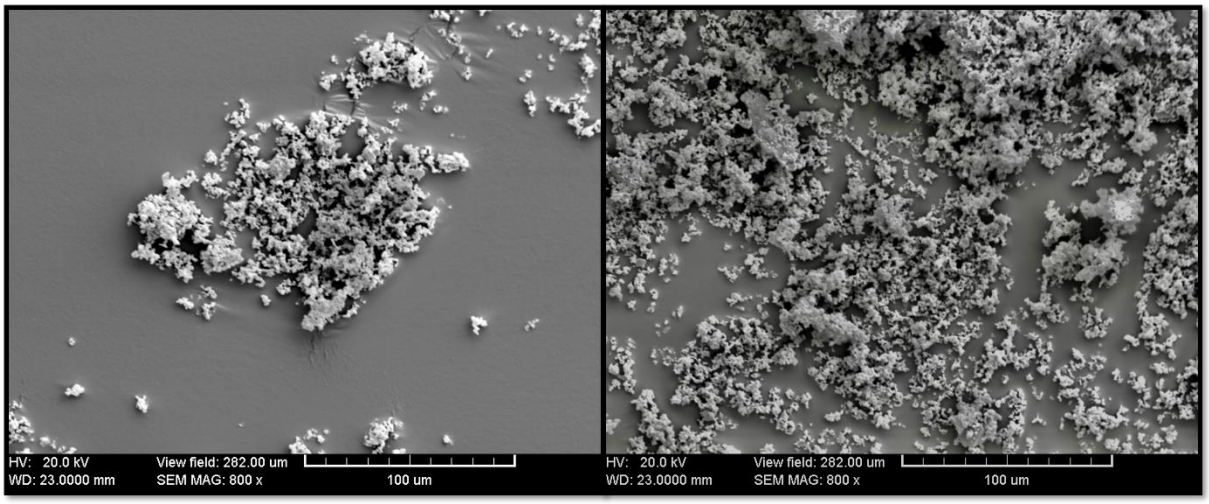

Figure S 11. SEM micrograph of $La_2Ni_{0.75}Co_{0.25}O_{4.08}$ before sintering at low magnification (800 x).

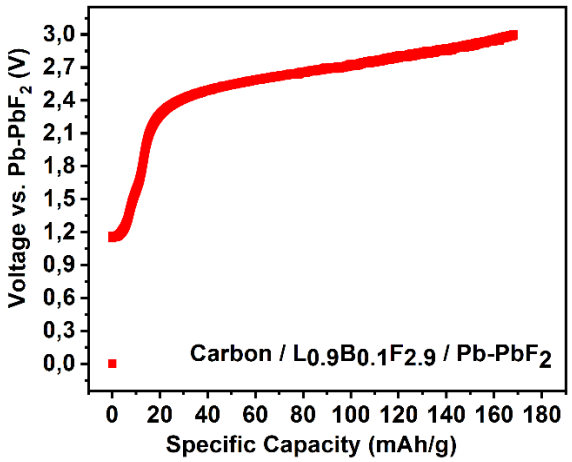

Figure S 12. Capacity-voltage curve for the cell operated only with carbon.